Available online at www.sciencedirect.com
SCIENCE DIRECT®
International Journal of Mass Spectrometry 230 (2003) 161–174
International Journal of Mass Spectrometry
www.elsevier.com/locate/ijms

Clustering and activation in reactions of $CoCp^+$ with hydrogen and methane

Catherine J. Carpenter [a], Petra A.M. van Koppen [a], Paul R. Kemper [a], John E. Bushnell [a], Patrick Weis [a,1], Jason K. Perry [b], Michael T. Bowers [a,*]

[a] *Department of Chemistry and Biochemistry, University of California, Santa Barbara, CA 93106, USA*
[b] *First Principles Research, 6327-C SW Capitol Hwy., PMB 250, Portland, OR 97239, USA*

Received 28 July 2003; accepted 19 August 2003

Abstract

Gas-phase clustering reactions of $CoCp^+$ with H_2 and with CH_4 were investigated using temperature-dependent equilibrium experiments. In both systems, the $CoCp^+$ ion was found to form strong interactions with two ligands. The first and second H_2 groups cluster to $CoCp^+$ with bond energies of 16.2 and 16.8 kcal/mol, respectively, while the first and second CH_4 groups cluster to $CoCp^+$ with bond energies of 24.1 and 12.1 kcal/mol, respectively. These bond energies are in good agreement with those determined by density functional theory (DFT). Molecular geometries for the four clusters determined with DFT are also presented. Weak experimental bond energies of 0.9 kcal/mol for the third H_2 and 2.2 kcal/mol for the third CH_4 clustering to $CoCp^+$ suggest these ligands occupy the second solvation shell of the ion. In addition to clustering in the methane system, H_2-elimination from $CoCp(CH_4)_2{}^+$ was observed. The mechanism for this reaction was investigated by collision-induced dissociation experiments and DFT, which suggest the predominate H_2-elimination product is (c-C_5H_6)Co^+–C_2H_5. Theory indicates that dehydrogenation requires the active participation of the Cp ring in the mechanism. Transfer of H and CH_3 groups to the C_5-ring ligand allows the metal center to avoid the high-energy Co(IV) oxidation state required when it forms two covalent bonds in addition to its interaction with a C_5-ring ligand.

Keywords: Sigma bond activation; Transition metal; Cobalt; Cyclopentadienyl ligand; Hydrogen; Methane; Density functional theory

1. Introduction

The activation of σ bonds in hydrogen and small alkanes has been the subject of many investigations [1]. One reason for this interest is the fact that alkanes, in the form oil and natural gas, make up an important feedstock for the chemical industry. Alkanes also happen to be comparatively unreactive compounds. For instance, ethylene and acetylene both have stronger C–H bonds than methane but are more reactive [1d]. While methods exist for the transformation of organic compounds with one functional group into compounds with a different functional group, alkanes remain a largely untapped source of precursors for more valuable compounds. In addition to this practical motivation for the study of σ-bond activation, there exists a more fundamental one. Sigma bonds are the most basic and prevalent bonds in the world of chemistry. An understanding of how they are formed and broken holds a fundamental interest to chemists. As the molecule with the simplest σ bond, hydrogen has been the focus of many activation studies [2].

Transition metals have been the traditional agent of σ-bond activation and their chemistry may hold the potential for a method of controlled activation. A limited number of investigations of reactions between neutral transition-metal atoms and small alkanes in the gas phase have been carried out [3]. Results show that in most case the neutral atoms are unreactive. This has been attributed to the repulsive, occupied valence ‘s’ orbitals of the neutrals. More reactive systems can be found by looking at transition metal cations. These systems have been widely studied, in part because they lend themselves to investigation using a variety of mass spectrometric techniques. In 1979, Allison, Freas and Ridge, discovered that transition metal ions oxidatively

* Corresponding author. Tel.: +1-805-893-2673; fax: +1-805-893-8703.
E-mail address: bowers@chem.ucsb.edu (M.T. Bowers).
[1] Present address: Institut für Physikalische Chemie, Universität Karlsruhe, Fritz-Haber-Weg, 76128 Karlsruhe, Germany.

1387-3806/$ – see front matter © 2003 Elsevier B.V. All rights reserved.
doi:10.1016/j.ijms.2003.08.010

insert into σ bonds of alkanes in the gas phase [4]. Since then, many research groups have shown that bare transition metal ions are reactive with larger alkanes [1a,b].

In the condensed phase, reactivity is achieved by binding transition metals with oxidizing ligands. In the early 1980s, several groups demonstrated the first examples of intermolecular alkane activation by a transition-metal complex. Rhodium and iridium complexes, $Cp^*M(PMe_3)$ (M = Rh, Ir) and Cp^*IrCO ($Cp^* = C_5Me_5$), have been found to activate C–H bonds in alkanes [5]. Complexes containing other metals, including Fe, Rh, Pd, Re, Os and Pt, have also been found to activate alkanes [6].

Several studies investigating the role of ligands in gas-phase reactions of transition-metal ions with hydrogen and small alkanes have been published. Guided ion-beam techniques [7] and FT-ICR [8] have been used to measure changes in reactivity, branching ratios and bond strengths as a result of transition-metal ion ligation by CO, H_2O, CH_2O and CH_2S. Our group has used temperature-dependent equilibrium experiments to investigate cluster-assisted activation in the Sc^+/H_2 and Ti^+/CH_4 systems [9]. In these systems, addition of multiple ligands to the metal ion is required to provide the energy necessary for insertion into an H–H or C–H bond.

The role of the Cp (η^5-C_5H_5) ligand in gas-phase ion–molecule reactions has received only limited attention [10,11]. The Cp ligand is ubiquitous in condensed-phase organotransition metal chemistry and plays a key role in some industrially important reactions [12]. It forms strong bonds to transition metals and is chemically resistant so it often functions in a passive role in reactions. We have reported in a communication that in gas-phase reactions, $CoCp^+$ is capable of eliminating H_2 when clustered with two methane ligands [13]. This was an interesting observation given that bare Co^+ only forms clusters with methane, with no elimination observed at thermal energies [14]. In fact, bare Co^+ does not activate σ bonds in ethane at thermal energies, even though the H_2-elimination reaction is exothermic by about 11 kcal/mol [15]. However, facile H_2-elimination from ethane is observed in thermal reactions with $CoCp^+$ [11]. In the $CpCo^+(CH_4)_2$ case, evidence presented in the communication suggests that H_2-elimination is only possible with the active participation of the Cp ring in the mechanism.

In this paper we will present the results obtained in temperature-dependent equilibrium studies of $CoCp^+$ clustering with both H_2 and CH_4.

$$CpCo^+(H_2)_{n-1} + H_2 \rightleftharpoons CpCo^+(H_2)_n \quad (1)$$

$$CpCo^+(CH_4)_{n-1} + CH_4 \rightleftharpoons CpCo^+(CH_4)_n \quad (2)$$

These experiments allow us to determine ΔH_0° and ΔS_0° for Reactions (1) and (2), for n = 1–3. To complement the experimental results, density functional theory (DFT) calculations were carried out to determine binding energies and geometric structures of the species involved in Reactions (1) and (2).

As with the bare Co^+/CH_4 system, when $CoCp^+$ reacts with a single CH_4 ligand, only clustering is observed. Unlike the bare Co^+ system though, when a second CH_4 is added, clustering (Reaction (3a), where M is a stabilizing collision partner) and cluster-assisted H_2-elimination (Reaction (3b)) are found to be competitive reaction channels.

$$CpCo^+ + 2CH_4 \rightleftharpoons [CoC_7H_{13}{}^+]^* \xrightarrow{M} CpCo^+(CH_4)_2 \quad (3a)$$

$$\rightarrow CoC_7H_{11}{}^+ + H_2 \quad (3b)$$

The structure of $CoC_7H_{11}{}^+$ formed in Reaction (3b) was investigated by measuring its fragmentation pattern in mass-analyzed ion kinetic energy spectroscopy (MIKES) and its H_2-loss kinetic energy release distribution (KERD). These results and extensive DFT calculations are used to establish the reaction mechanism for H_2 loss from double methane addition to $CoCp^+$.

2. Methods

2.1. Temperature-dependent equilibrium experiments

Temperature-dependent equilibrium experiments were carried out to investigate the clustering of H_2 and CH_4 with $CoCp^+$ (Reactions (1) and (2), respectively). The method used has been previously described in detail [9a,16] and only the specifics of this experiment will be discussed here. $CoCp^+$ ions were formed by electron impact (EI) on $CoCp(CO)_2$, mass-selected with a quadrupole and injected into a reaction cell containing several Torr of H_2 or CH_4. Ions drifted through the cell under the influence of a weak electric field. This electric field does not measurably perturb the thermal energies of the ions. The reaction time of $CoCp^+$ clustering with H_2 or CH_4 is proportional to P/V, where P is the pressure in the reaction cell and V is the drift voltage, and can be varied to ensure equilibrium of Reaction (1) or (2) is established. As the ions exited the reaction cell, they were analyzed by a second quadrupole and detected. The temperature of the reaction cell was varied over a range of 80–800 K and the equilibrium constants, K, were determined as a function of temperature using Eq. (4).

$$K = \frac{CoCp^+(L)_n(760)}{CoCp^+(L)_{n-1}P_L} \quad (4)$$

In this expression, L represents either H_2 or CH_4. The value $CoCp^+(L)_n$ is the intensity of the product ion and $CoCp^+(L)_{n-1}$ is the intensity of the reactant ion. P_L is the pressure of the neutral reactant in Torr and the factor of 760 normalizes the equilibrium constant to standard-state conditions. The equilibrium constants were then used to calculate standard-state free energies, ΔG_T°, using Eq. (5).

$$\Delta G_T^\circ = -RT \ln K \quad (5)$$

Enthalpies and entropies for Reactions (1) and (2) were determined by plotting ΔG°_T versus temperature, T, which yields a line with an intercept equal to ΔH°_T and a slope equal to $-\Delta S^\circ_T$ (Eq. (6)).

$$\Delta G^\circ_T = \Delta H^\circ_T - T\,\Delta S^\circ_T \quad (6)$$

The values determined by this method are valid over the temperature range of the experiment. Bond dissociation energies at $T = 0$ K ($-\Delta H^\circ_0$) were obtained by fitting the experimental data using a statistical mechanical model based on vibrational frequencies and molecular geometries determined from DFT calculations.

2.2. MIKES experiments

To investigate the structure of the $CoC_7H_{11}^+$ ion formed by reaction of $CoCp^+$ with methane, we performed metastable and collision-induced dissociation (CID) ion kinetic energy studies using a reverse-geometry double-focusing mass spectrometer (V.G. ZAB-2F) [17]. The $CoC_7H_{11}^+$ ions were generated by two different methods: Reaction (3b) and by direct clustering with ethane (Reaction (7)).

$$CpCo^+C_2H_6 \rightleftharpoons [CoC_7H_{11}^+]^* \xrightarrow{M} CoC_7H_{11}^+ \quad (7a)$$

$$\rightarrow CoC_7H_9^+ + H_2 \quad (7b)$$

For each method, $CoCp^+$ was formed by EI on $CoCp(CO)_2$ in the ion source. The ions exiting the source were accelerated to 8 keV and $CoC_7H_{11}^+$ was mass-selected by the magnetic sector. Decomposition occurred either metastably or was induced by collision with helium in the field-free region between the magnetic and electric sectors.

Full-scale mass-analyzed ion kinetic energy spectra (MIKES) for both metastable dissociation and CID were obtained by scanning the electric sector plate voltages to pass fragment ions with kinetic energies between 0 and 8000 eV. In the resulting spectra, peaks are observed at energies corresponding to the fragments formed during dissociation. These experiments were repeated for $CoC_7H_5D_6^+$ formed in reactions of $CoCp^+$ with CD_4 (as in Reaction (3b)) and C_2D_6 (as in Reaction (7)). Product KERDs for H_2 loss from $CoC_7H_{11}^+$ formed in Reactions (3b) and (7) were obtained by narrowing the electric sector scan for the $CoC_7H_9^+$ fragment formed under metastable conditions. These distributions were converted from the lab frame of reference to the center-of-mass frame of reference using the TRAMP method [18].

All chemicals used in these experiments and in the equilibrium experiments described in the previous section were obtained commercially and were purified only by freeze–pump–thaw cycles to remove noncondensable gases.

2.3. Theory

Species involved in Reactions (1), (2) and (3) were examined by DFT with the B3LYP functional [19] using JAGUAR 5.0 [20]. Geometry optimizations were first performed using JAGUAR's LACVP basis set. This is composed of Hay and Wadt's Ne core ECP in conjunction with their standard valence double-ζ basis set [21a] for Co and a 6-31G** basis set [21b] for C and H. Final single-point energies were evaluated using JAGUAR's LACV3P basis set, which is a valence triple-ζ contraction of the Hay and Wadt basis set for Co and a 6-311+G** basis set [21c,d] for C and H. Thorough examination of the complexation of H_2 to $CoCp^+$ strongly suggested that the B3LYP functional is biased toward the high-spin quartet state. Data on the doublet state of $CoCp^+$ and its various complexes were more consistent with experiment. Thus, in this work we restrict ourselves to calculations on the doublet potential energy surface for the reaction of $CoCp^+$ with two CH_4 molecules.

3. Results

3.1. Equilibrium experiment

Standard-state free energies, ΔG°_T, were determined, as described in the Methods section, over a wide range of temperatures for sequential clustering of H_2 and CH_4 to the $CoCp^+$ core ion. These data are plotted in Fig. 1. In each system, a maximum of three ligands were found to cluster to $CoCp^+$. The ΔH°_T and ΔS°_T values determined from these plots are collected in Table 1 for clustering with H_2 and Table 2 for CH_4. In both systems, the first two ligands are relatively strongly bound, 16.2 and 16.8 kcal/mol for the first and second H_2 ligand, respectively, and 24.1 and 12.1 kcal/mol for the first and second CH_4 ligand, respectively. The third ligand in each case is weakly bound, 0.9 kcal/mol for H_2 and 2.2 kcal/mol for CH_4. The entropies follow a similar pattern. There is a substantial drop in entropy for addition of the first two ligands, while the drop for the third is significantly smaller in both the $CoCp^+/H_2$ and $CoCp^+/CH_4$ systems.

3.2. MIKES experiment

The metastable MIKES for $CoC_7H_{11}^+$ formed by both Reactions (3b) and (7) are shown in Fig. 2. As the spectra indicate, the only significant fragment produced under metastable conditions in both cases is $CoC_7H_9^+$, due to H_2 loss. More fragmentation is observed under CID conditions, Fig. 3. For $CoC_7H_{11}^+$ formed from $CoCp^+ + C_2H_6$ (Reaction (7)), the most significant ionic fragments produced upon CID are Co^+, $CoCp^+$ and $CpCo^+(C_2H_4)$ (Fig. 3a). The corresponding spectrum for $CoCp^+ + C_2D_6$ (data not shown) indicated a similar fragmentation pattern, with Co^+,

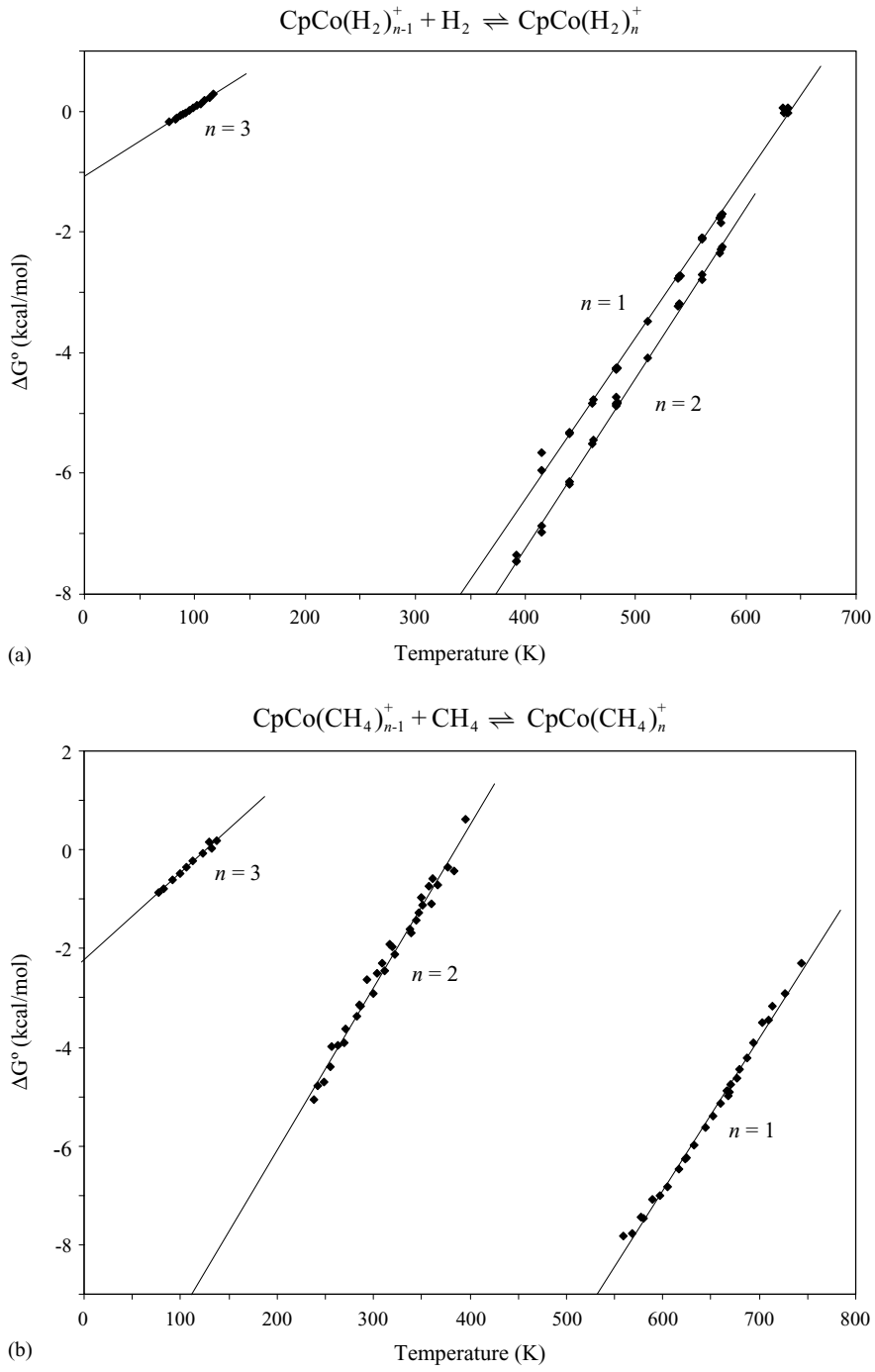

Fig. 1. Plot of experimental ΔG° vs. temperature for the association reactions $CpCo^+(L)_{n-1} + L \rightleftharpoons CpCo^+(L)_n$ for (a) $L = H_2$ and (b) $L = CH_4$.

Table 1
Experimental ΔH_T° and ΔS_T° values at temperature T and experimental and theoretical ΔH_0° values at 0 K for the reaction: $(Cp)Co^+(H_2)_{n-1} + H_2 \rightleftharpoons (Cp)Co^+(H_2)_n$

n	Experiment				Theory
	$-\Delta H_T^\circ$ (kcal/mol)	$-\Delta S_T^\circ$ (cal/mol K)	T(K)[a]	$-\Delta H_0^\circ$ (kcal/mol)	$-\Delta H_0^\circ$ (kcal/mol)
1	17.1 ± 0.9	26.7 ± 1.7	525 ± 100	16.2	15.1
2	18.5 ± 1.1	28.2 ± 2.2	490 ± 100	16.8	16.6
3	1.1 ± 0.1	11.6 ± 1.1	100 ± 250	0.9	–

[a] Experimental temperature range.

Table 2
Experimental ΔH°_{T} and ΔS°_{T} values at temperature T and experimental and theoretical ΔH°_{0} values at 0 K for the reaction: $(Cp)Co^{+}(CH_4)_{n-1} + CH_4 \rightleftharpoons (Cp)Co^{+}(CH_4)_n$

n	Experiment				Theory
	$-\Delta H^{\circ}_{T}$ (kcal/mol)	$-\Delta S^{\circ}_{T}$ (cal/mol K)	T(K)[a]	$-\Delta H^{\circ}_{0}$ (kcal/mol)	$-\Delta H^{\circ}_{0}$ (kcal/mol)
1	25.4 ± 1.9	30.8 ± 2.7	650 ± 100	24.1	18.7
2	12.6 ± 1.1	32.9 ± 3.9	325 ± 750	12.1	11.4
3	2.2 ± 0.1	17.8 ± 1.3	100 ± 250	2.2	–

[a] Experimental temperature range.

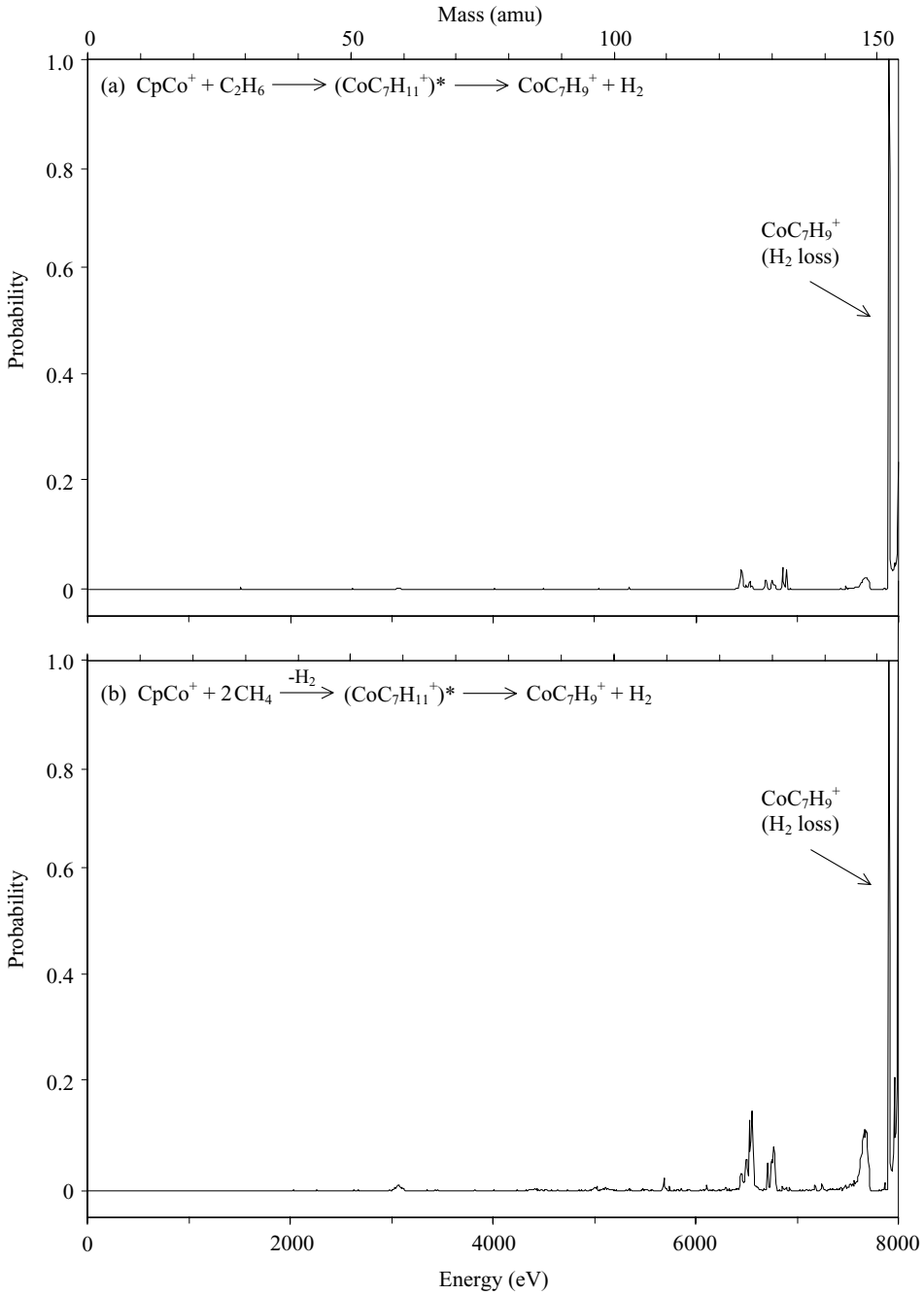

Fig. 2. Kinetic-energy/mass spectra for metastable dissociation of $CoC_7H_{11}^{+}$ formed by (a) reaction of $CoCp^{+}$ with C_2H_6 and (b) reaction of $CoCp^{+}$ with $2CH_4$ followed by H_2-elimination. The peaks observed between 4000 eV and the H_2-loss peak are artifacts.

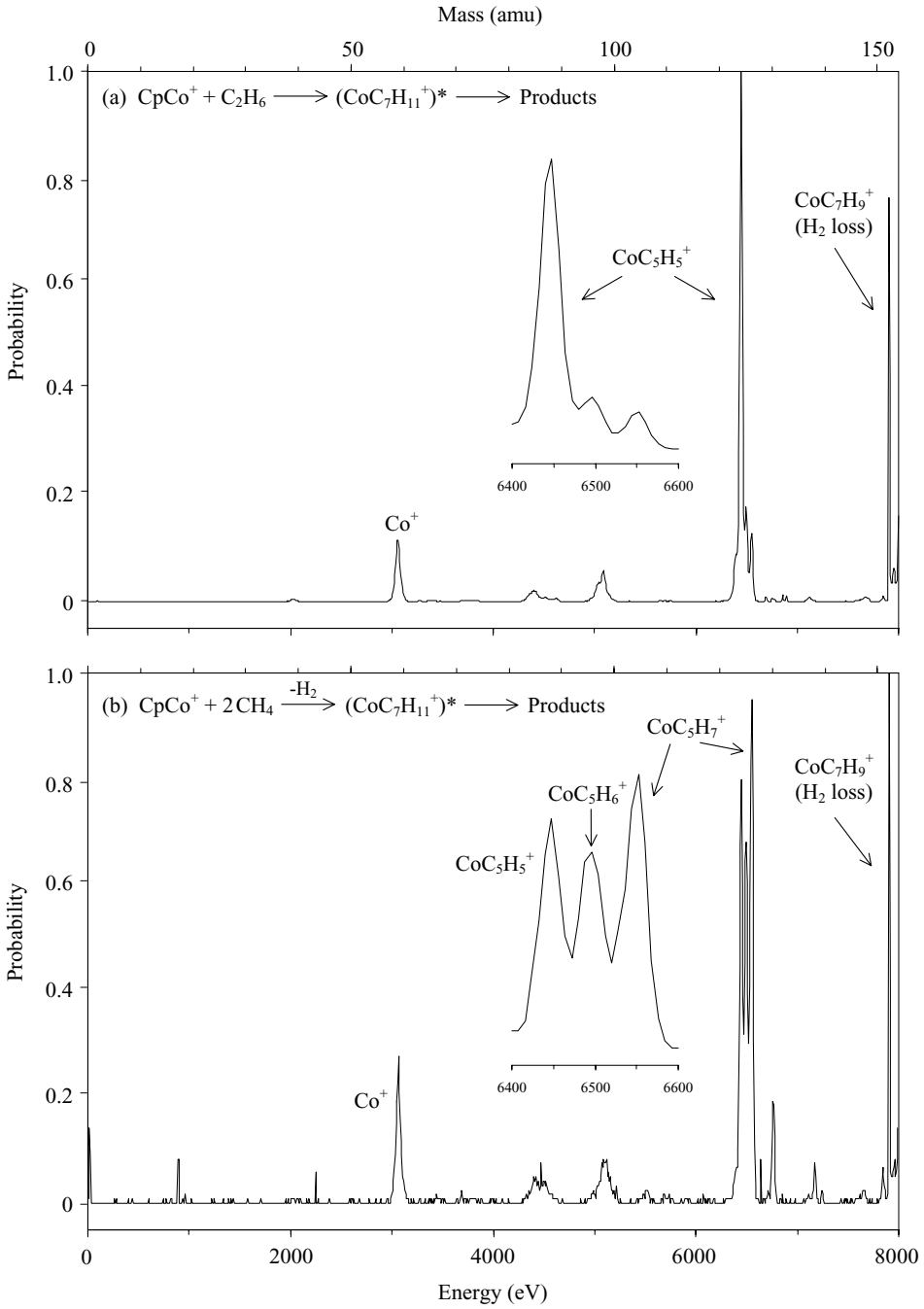

Fig. 3. Kinetic-energy/mass spectra for collision-induced dissociation of $CoC_7H_{11}^+$ formed by (a) reaction of $CoCp^+$ with C_2H_6 and (b) reaction of $CoCp^+$ with $2CH_4$ followed by H_2-elimination. Insets show an enlargement of each spectrum in an energy range of 6400–6600 eV.

$CoCp^+$ and $CpCo^+(C_2D_4)$. No HD or H_2 loss is observed for $CoCp^+$ reacting with C_2D_6.

Just as in metastable dissociation, CID of $CoC_7H_{11}^+$ formed by sequential reaction of $CoCp^+$ with two CH_4 molecules followed by H_2-elimination (Reaction (3b)) shows a significant peak corresponding to H_2 loss. In addition, as seen in the CID spectrum for $CoC_7H_{11}^+$ formed from $CoCp^+ + C_2H_6$, there are strong peaks for Co^+ and $CoC_5H_5^+$. In contrast, however, the CID spectrum of $CoC_7H_{11}^+$ formed by H_2 loss from $CoCp^+ + 2CH_4$ in Fig. 3b shows significant peaks corresponding to $CoC_5H_6^+$ and $CoC_5H_7^+$. The fragmentation of $CoC_7H_5D_6^+$ formed by D_2 loss from $CoCp^+ + 2CD_4$ was also examined (data not shown). Although the signals for the deuterated analog were weaker, it appears to lose D_2, HD and H_2.

KERDs for H_2 loss from $CoC_7H_{11}^+$ formed in Reactions (3b) and (7) are shown in Fig. 4. The two distributions are nearly identical. In both cases, the H_2-loss KERD is an

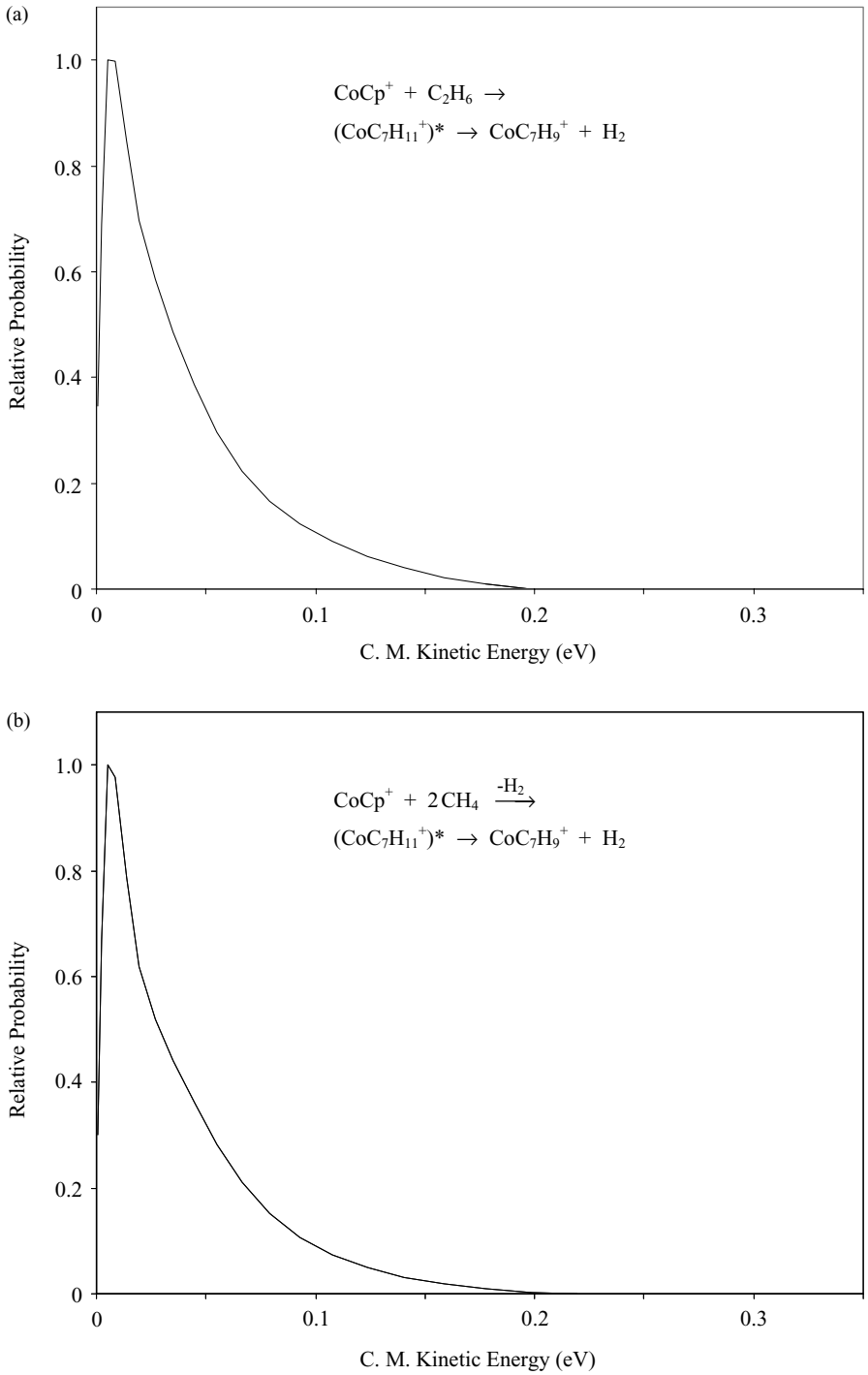

Fig. 4. Experimental KERDs for metastable H_2 loss from $CoC_7H_{11}^+$ formed by (a) reaction of $CoCp^+$ with C_2H_6 and (b) reaction of $CoCp^+$ with $2CH_4$ followed by H_2-elimination.

average of several sets of scans taken on different occasions with main-beam lab-frame-of-reference resolutions ranging from 1.4 to 2.0 eV FWHM. The center-of-mass distribution for H_2 loss from $CoC_7H_{11}^+$ formed in Reaction (7) has an average kinetic energy release of 39 ± 5 meV. The KERD for H_2 loss from $CoC_7H_{11}^+$ formed in Reaction (3b) has an average release of 38 ± 5 meV. Both KERDs appear to be statistical, indicating no energy barrier in the exit channel for formation of products is present in either reaction [22].

3.3. Theory

The lowest-energy doublet structure for $CoCp^+$ determined in the DFT calculations is shown in Fig. 5. The

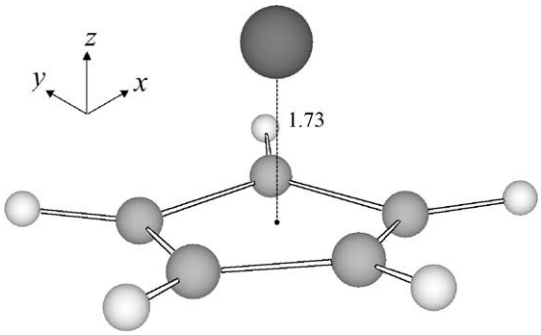

Fig. 5. Geometry of the $CoCp^+$ determined by DFT. The distance between Co and the Cp group is given in Å. Cobalt atoms are shown in dark gray, carbons in medium gray and hydrogens in light gray.

Cp ligand is a strong electron-withdrawing group and thus oxidizes the metal to form a Co(II) center. The Cp ring is almost planar with the Co atom approximately 1.73 Å away.

Several structures for the $CpCo^+(H_2)$ doublet were examined. The lowest-energy structure is shown in Fig. 6. The Cp ring is 1.76 Å away from Co and the H_2 ligand is 1.66 Å away from Co. The H_2 group forms an angle of 128.3° with the Cp ligand, while the H_2 bond is approximately parallel to the plane of the Cp ring. The H_2 bond length is 0.79 Å, 0.05 Å longer than the bond in free H_2. The other structures considered, where H_2 is reoriented relative to the rest of the complex, all have geometrical characteristics similar to those described for the lowest-energy structure. They are 2.0–3.6 kcal/mol higher in energy than the structure shown in Fig. 6.

The structure for $CoCp^+$ clustering with two H_2 ligands was also investigated. Again, several possible structures were considered for the doublet $CpCo^+(H_2)_2$. The lowest-energy structure is shown in Fig. 6. The Cp ring is 1.78 Å away from Co and the H_2 ligands are 1.67 Å away from Co. The H_2 groups from an angle of 99.1° with one another and an angle of 127.1° with the Cp ligand and are tilted at an angle of approximately 16° relative to the Cp plane. The H_2 bonds are both 0.79 Å long. Structures with different orientations of the H_2 ligands are 0.7–2.3 kcal/mol higher in energy.

The lowest-energy structures for $CpCo^+(CH_4)$ and $CpCo^+(CH_4)_2$ are shown in Fig. 7. For the $CpCo^+(CH_4)$ cluster, the Cp ring is 1.74 Å away from Co. The methane group coordinates to Co with an η^3 configuration where the carbon atom is 2.17 Å away from cobalt. Methane forms an angle of 163.7° with the Cp ring. In the lowest-energy $CpCo^+(CH_4)_2$ structure, the Cp ring is 1.76 Å away from Co. Both methane groups coordinate to cobalt with an η^2 configuration where the carbon atoms are 2.35 Å away from cobalt. The two methane ligands form an angle of 89.9° with each other and are both at an angle of 135.1° relative to the Cp ring.

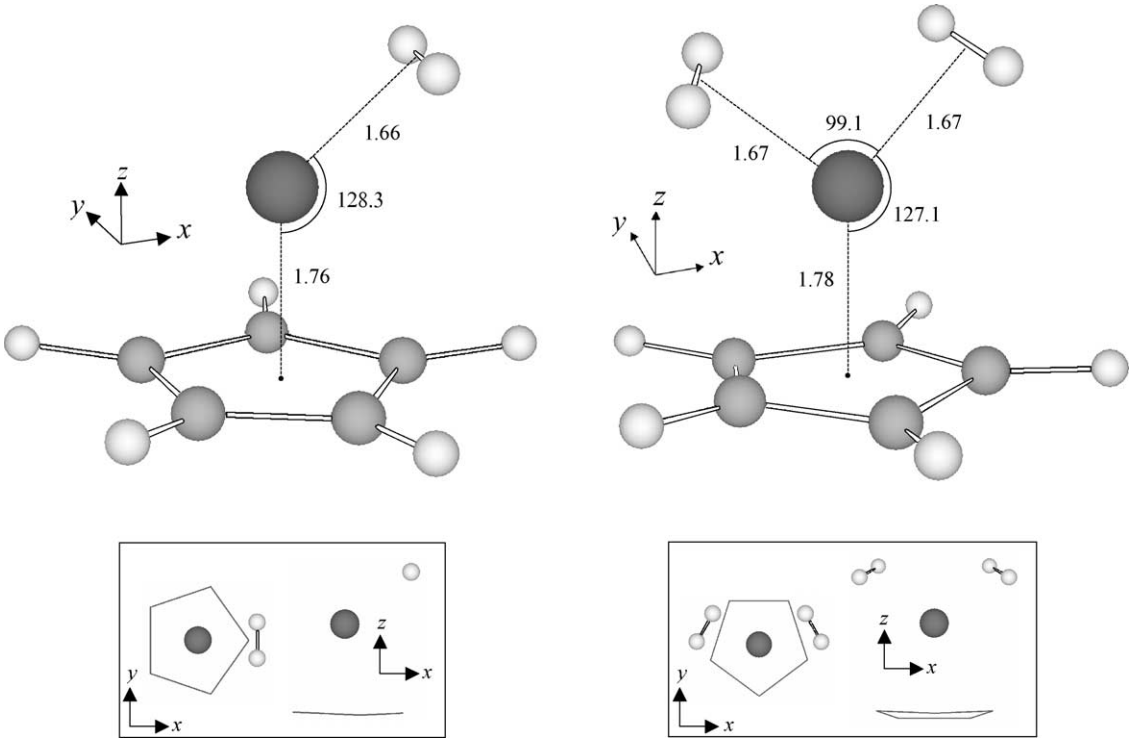

Fig. 6. Geometries of the $CpCo^+(H_2)$ and $CpCo^+(H_2)_2$ clusters determined by DFT. Selected intramolecular distances and angles are given in Å and degrees (°), respectively. Cobalt atoms are shown in dark gray, carbons in medium gray and hydrogens in light gray. Insets show the orientation of the H_2 ligand(s) relative to the Cp ring. In the $CpCo^+(H_2)_2$ structure, the H_2 ligands are in the same plane as one another and are tilted approximately 16° with respect to the plane of the Cp ring.

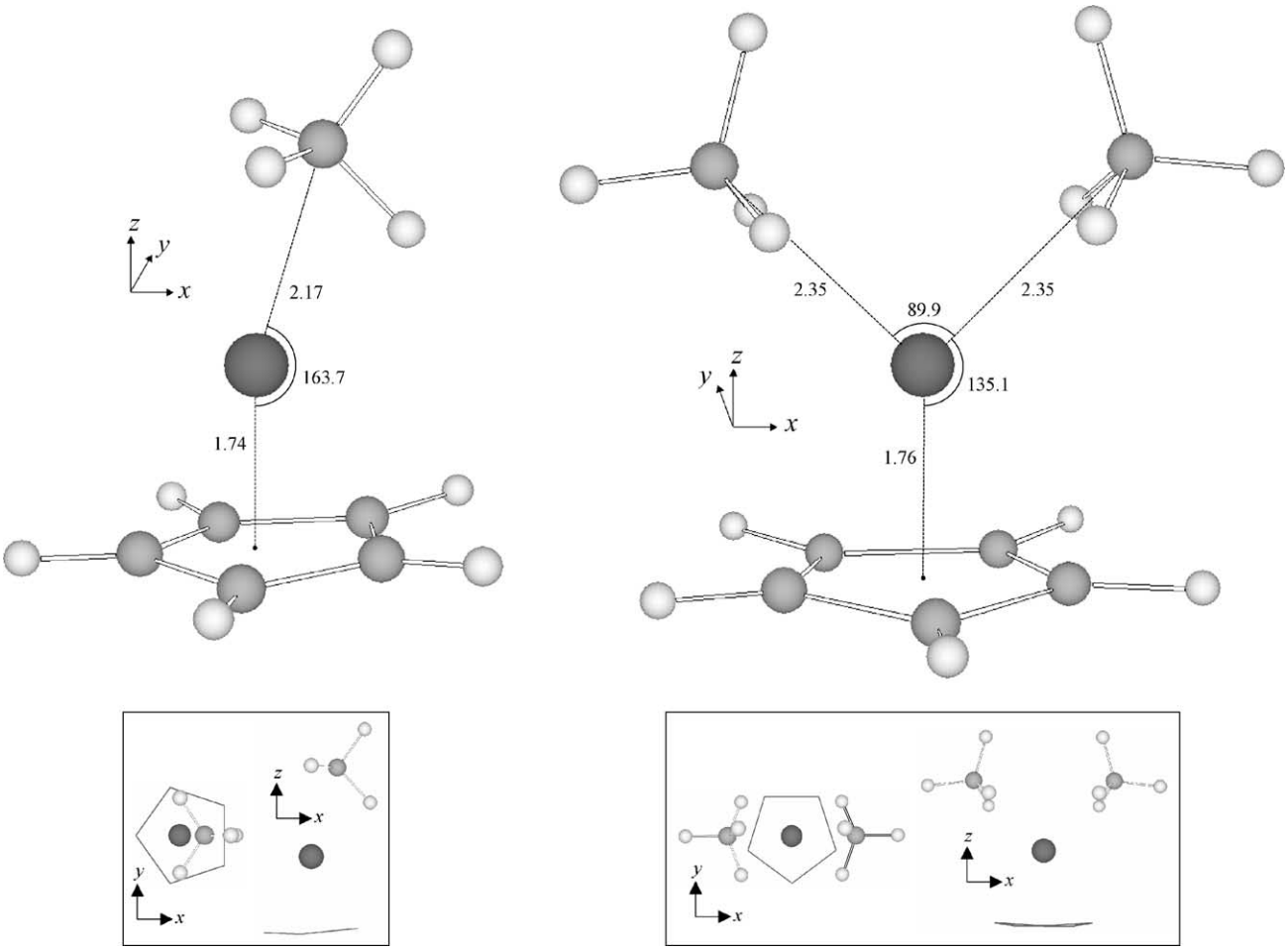

Fig. 7. Geometries of the $CpCo^+(CH_4)$ and $CpCo^+(CH_4)_2$ clusters determined by DFT. Selected intramolecular distances and angles are given in Å and degrees (°), respectively. Cobalt atoms are shown in dark gray, carbons in medium gray and hydrogens in light gray. Insets show the orientation of the CH_4 ligand(s) relative to the Cp ring.

Using the spatial orientations indicated in the Figs. 5–7, the Co^{2+} electron configuration in the $CpCo^+(H_2)_{1,2}$ and $CpCo^+(CH_4)_{1,2}$ clusters is $(d_{z^2})^2(d_{x^2-y^2})^2(d_{xy})^2(d_{yz})^1(d_{xz})^0$. Thus the Cp ring destabilizes the Co π orbitals (d_{xz} and d_{yz}) and the ligands coordinate to the empty π orbital (d_{xz}).

The $CpCo^+$–(H_2) and $Cp(H_2)Co^+$–(H_2) bond energies ($-\Delta H_0^\circ$ for Reaction (1)) determined with DFT are shown in Table 1. The first H_2 ligand is bound by 15.1 kcal/mol, while the second is slightly more strongly bound at 16.6 kcal/mol. These numbers are in good agreement with the bond energies determined experimentally. The $CpCo^+$–(CH_4) and $Cp(CH_4)Co^+$–(CH_4) bond energies ($-\Delta H_0^\circ$ for Reaction (2)) determined with DFT are listed in Table 2. Calculations show the first methane ligand to be bound by 18.7 kcal/mol. While the second H_2 ligand in the $CpCo^+(H_2)_n$ system is bound more strongly than the first H_2 group by 1.5 kcal/mol, the second methane in the $CpCo^+(CH_4)_n$ system is bound significantly more weakly, at 11.4 kcal/mol, compared to the first methane ligand. The agreement between the experimental and theoretical $CpCo^+(CH_4)_{1,2}$ bond energies is not as good as in the $CpCo^+(H_2)_{1,2}$ system but theory does predict the observed drop between the first and second CH_4 bond energies.

4. Discussion

It is well known that bare transition metal ions are able to activate σ bonds in propane and larger alkanes [15,23]. Here, we report our experimental evidence that the ligand effect imposed by the cyclopentadienyl group on a cobalt ion allows it to induce H_2-elimination from two methane molecules (Reaction (3b)). This reaction has been observed in temperature-dependent equilibrium studies and MIKES experiments. The mechanism is further investigated by DFT as described below.

4.1. $CpCo^+(H_2)_n$ and $CpCo^+(CH_4)_n$ bond energies

The experimental and theoretical bond energies for the $CpCo^+(H_2)_n$ and $CpCo^+(CH_4)_n$ clusters determined in this study are listed in Table 3. For comparison, experimental

Table 3
Experimental and theoretical bond dissociation energies in kcal/mol for $Co^+(H_2)_{1,2}$, $Co^+(CH_4)_{1,2}$, $CpCo^+(H_2)_{1,2}$ and $CpCo^+(CH_4)_{1,2}$

	Equilibrium	Ion beam	DFT		Equilibrium	DFT
Co^+–(H_2)	18.2 ± 1.0[a]	17.5 ± 2.3[c]	18.6[e]			
$(H_2)Co^+$–(H_2)	17.0 ± 0.7[a]	–	16.6[e]	$CpCo^+$–(H_2)	16.2	15.1
$(H_2)_2Co^+$–(H_2)	9.6 ± 0.5[a]	–	8.4[e]	$(H_2)CpCo^+$–(H_2)	16.8	16.6
$(H_2)_3Co^+$–(H_2)	9.6 ± 0.6[a]	–	7.3[e]	$(H_2)_2CpCo^+$–(H_2)	0.9	–
Co^+–(CH_4)	23.1[b]	21.4 ± 1.4[d]	22.9[b]			
$(CH_4)Co^+$–(CH_4)	25.3[b]	23.1 ± 1.2[d]	22.1[b]	$CpCo^+$–(CH_4)	24.1	18.7
$(CH_4)_2Co^+$–(CH_4)	7.3[b]	9.4 ± 1.2[d]	5.4[b]	$(CH_4)CpCo^+$–(CH_4)	12.1	11.4
$(CH_4)_3Co^+$–(CH_4)	5.2[b]	15.4 ± 1.4[d]	2.2[b]	$(CH_4)_2CpCo^+$–(CH_4)	2.2	–

[a] From [24a].
[b] From [14b].
[c] From [24b].
[d] From [14a].
[e] From [25].

and theoretical bond energies for bare Co^+ clustering with H_2 and CH_4 are also shown. For clustering of both H_2 and CH_4 to bare Co^+, a pair-wise behavior was observed experimentally and theoretically for the bond energies. These patterns have been explained based on the geometries of the clusters and the hybridization of the Co^+ valence orbitals [14,24,25]. For H_2, the first solvation shell fills with six ligands in a pseudo-octahedral structure, while for the larger CH_4 group, four ligands occupy the first solvation shell in a pseudo-planar D_{2h} symmetry (two shorter and two longer Co^+–CH_4 bonds).

Examination of the bond energies and entropy changes for H_2 clustering with $CoCp^+$ (Table 1) shows that the $CoCp^+$ core interacts strongly with only two H_2 ligands. In other words, the Cp ring and two H_2 ligands fill up the first solvation shell of Co^+. The first two H_2 groups bind almost as strongly to $CoCp^+$ as to bare Co^+ (Table 3). The third H_2 ligand is bound by less than 1 kcal/mol. The values for ΔS°_T listed in Table 1 also indicate that $CoCp^+$ does not have a strong interaction with the third H_2 molecule.

The substantial drops in entropy for the additions of the first and second H_2 are consistent with the first two ligands being locked relatively tightly in place, resulting in the substantial loss of movement for these groups. On the other hand, the third, weakly bound H_2 ligand has a much smaller drop in entropy, consistent with a less restricted interaction. The idea that the first solvation shell is filled for $CpCo^+(H_2)_2$ is consistent with the molecular geometry obtained in the DFT calculations. Fig. 6 shows that the Cp ring and two H_2 ligands leave little room for an additional ligand to approach the metal center.

A similar pattern is observed for the $CpCo^+(CH_4)_n$ system. The first CH_4 ligand forms a relatively strong bond to $CoCp^+$ at 24.1 kcal/mol (Table 3). This bond strength is similar to what is observed for the first two CH_4 ligands binding to bare Co^+. However, there is a substantial drop in bond energy to 12.1 kcal/mol for the second methane clustering to $CoCp^+$. This is consistent with the structures for $CpCo^+(CH_4)$ and $CpCo^+(CH_4)_2$ determined by DFT. Fig. 7 shows that when just one CH_4 ligand clusters to $CoCp^+$, the methane carbon is 2.17 Å away from the cobalt atom. When a second methane ligand is added, both ligands pull out so they are 2.35 Å away from the cobalt center, consistent with the weaker $Cp(CH_4)Co^+$–(CH_4) bond. The third methane ligand was found to be bound by only 2.2 kcal/mol and just as in the $CpCo^+(H_2)_n$ system, the entropy change for the addition of this ligand is significantly smaller than for the first two CH_4 ligands, indicating that it is part of the second solvation shell.

4.2. Loss of H_2 from $CpCo^+(CH_4)_2$ in equilibrium experiments

When $CoCp^+$ is injected into the reaction cell containing methane and equilibrium is established, mass spectra of ions exiting the cell show a peak two mass units below the $CpCo^+(CH_4)_2$ peak (data not shown). This peak at m/z = 154 corresponds to a species with the formula $CoC_7H_{11}^+$ that we attribute to H_2 loss from $CpCo^+(CH_4)_2$ (Reaction (3b)).[2] The propensity to form $CoC_7H_{11}^+$ depended strongly on the cell temperature and pressure. Ratios of the intensities of the m/z = 154 ion to the m/z = 156 ion ranged between 0 and almost 1. Hence, while H_2 loss was not a major reaction channel for the $[CpCo^+(CH_4)_2]^*$ intermediate under all conditions, it was observed. This remarkable observation prompted further study of the reaction using MIKES.

4.3. Metastable and collision-induced dissociation

The loss of H_2 from $CpCo^+(CH_4)_2$ (Reaction (3b)) was also observed in the MIKES experiments. The structure of the H_2-loss product was investigated by comparing its fragmentation pattern with that of $CpCo^+(C_2H_6)$ formed in Re-

[2] The peak observed at m/z = 154 is not believed to be due to $CpCo^+(CH_2)(CH_4)$ because activation of a single methane by $CoCp^+$ (i.e., formation of $CpCo^+(CH_2)$) was not observed under any of our experimental conditions.

action (7). Under metastable conditions, H_2 loss is the predominant reaction for $CoC_7H_{11}^+$ formed by either Reaction (3b) or (7). This can be seen in the spectra shown in Fig. 2. However, more structural information can be gained by examining the CID spectra.

Fig. 3 shows that the fragmentation patterns for $CoC_7H_{11}^+$ formed by the two methods are significantly different. For $CoC_7H_{11}^+$ formed by Reaction (7), the large C_2H_6-loss peak is consistent with an ethane complex, $CpCo^+(C_2H_6)$, for the structure of the $CoC_7H_{11}^+$ precursor ion. In contrast, the spectrum obtained for $CoC_7H_{11}^+$ produced by H_2 loss from the $CpCo^+(CH_4)_2$ cluster has a significant peaks corresponding to the masses of $CoC_5H_6^+$ and $CoC_5H_7^+$. These results suggest the structures of the $CoC_7H_{11}^+$ ions formed by Reactions (3b) and (7) are different.

High-resolution scans revealed multiple peaks at the nominal mass of 154 in both systems. It is possible that some of these peaks are due to the presence of species such as the ^{13}C isotopes of $CpCo(CO)(H)^+$ and $CpCoC_2H_5^+$, which are both slightly lighter than the desired species $CoC_7H_{11}^+$. Although the fragmentation patterns seen in Fig. 3 were obtained using the best practical resolution possible (<2 eV FWHM) and mass-selecting the peak for the heaviest isotope present, we cannot completely rule out some possible contribution of these undesired isotopes to the fragmentation patterns observed in Fig. 3.[3]

As noted earlier, ion equilibrium studies of H_2 and CH_4 clustering indicate that the first solvation shell of $CoCp^+$ can only accommodate two additional ligands. Thus, it is probable that the intermediate $CoC_7H_{13}^+$ species leading to the formation of the products $CoC_7H_{11}^+$ and H_2 (Reaction (3b)) has at most three ligands coordinated to the cobalt ion. Because this intermediate eliminates dihydrogen, one of the ligands is most probably H_2. A second ligand must be a five-carbon ring species. Based on these assumptions, the two most reasonable structures for the $CoC_7H_{11}^+$ product ion formed in Reaction (3b) are $CpCo^+(C_2H_6)$ and $(c\text{-}C_5H_6)Co^+–C_2H_5$. Exclusive formation of the ethane complex, $CpCo^+(C_2H_6)$, can be ruled out by comparing the CID fragmentation patterns in Fig. 3. Formation of a significant amount of $(c\text{-}C_5H_6)Co^+–C_2H_5$ is consistent with the strong peaks for $CoC_5H_6^+$ and $CoC_5H_7^+$ observed in the CID spectrum (Fig. 3b). Collisional activation of $(c\text{-}C_5H_6)Co^+–C_2H_5$ would most likely result in loss of both C_2H_5 and C_2H_4.

4.4. H_2-loss KERDs

We have also measured the KERDs for H_2 loss from metastable $CoC_7H_{11}^+$ formed by the two methods (Reactions (3b) and (7)). These distributions are shown in Fig. 4. As in the full-scale MIKES measurements, the peak with the highest m/z at mass 154 was used to measure the H_2-loss KERD shown in Fig. 4b.

The two H_2-loss KERDs are nearly identical despite the fact that internal energy and angular momentum distributions of $CoC_7H_{11}^+$ formed by the two different methods may be quite different. In the case of $CoC_7H_{11}^+$ formation from $CoCp^+ + C_2H_6$, ion source pressures for measurement of the H_2-loss KERDs were less than 10 mTorr. This ensures single-collision conditions for the formation of the adduct and therefore no collisional stabilization. Since formation of $CoC_7H_{11}^+$ from $CoCp^+ + 2CH_4$ was carried out at source pressures of approximately 10–40 mTorr and H_2 must be lost from the $CpCo^+(CH_4)_2$ collision complex to form $CoC_7H_{11}^+$, the internal energy and angular momentum distributions of $CoC_7H_{11}^+$ are unknown. The difference in energy distributions is offset by the fact that only $CoC_7H_{11}^+$ ions with lifetimes of 10–15 μs are observed in our experiment. This time window only allows detection of fragments arising from parent ions associated with a small fraction of the total energy distribution. Nonetheless, the fact that the KERDs are nearly identical is strong evidence of the existence of a common precursor for H_2 loss from the $CoC_7H_{11}^+$ ions formed in Reactions (3b) and (7). This is not surprising since metastable reactions by definition occur at high energy (above the dissociation threshold) suggesting the two products of Reactions (3b) and (7) could isomerize before losing H_2. The fact that the KERDs are identical also indicates a ^{13}C isotope of either $CpCo(CO)(H)^+$ or $CpCoC_2H_5^+$ does not contribute to the metastable H_2 loss in the CH_4 experiment.

4.5. DFT investigation of mechanism for H_2 loss from $CpCo^+(CH_4)_2$

In a communication [13] on this work we proposed a mechanism for H_2 loss from $CpCo^+(CH_4)_2$ that involves the transfer of a hydrogen atom from methane to the Cp ring (Scheme 1). For this preliminary mechanism, we had located the initial transition state which is associated with the transfer of a hydrogen atom from one of the methane

[3] It is possible in the $CoCp^+/CH_4$ system that the peak at $m/z = 154$ may be (partially) due to the carbon-13 isotope of $CpCoC_2H_5^+$ formed by reaction of the precursor compound $CpCo(CO)_2$ and $C_2H_5^+$ formed in the ionized methane plasma. Formation of $C_2H_5^+$ under these conditions is possible in our MIKES experiment performed on the reverse-geometry double-focusing mass spectrometer where $CoCp^+$ is formed by EI on $CpCo(CO)_2$ in the presence of methane. However, literature thermochemistry indicates formation of $CpCoC_2H_5^+$ from $CpCo(CO)_2$ and $C_2H_5^+$ is endothermic by ∼10 kcal/mol. The mechanism for this reaction also needs to be considered. It most likely involves passage through a high-energy transition state and therefore is not likely to occur. Even if formation of the ^{13}C isotope of $CpCoC_2H_5^+$ is a factor in the $CoCp^+ + 2CH_4$ system, it should also be present in the $CoCp^+ + C_2H_6$ system since the $C_2H_5^+$ ion is also formed in EI on C_2H_6.
In the temperature-dependent equilibrium experiments, $CoCp^+$ is again formed by EI but not in the presence of methane. $CoCp^+$ is formed in the ion source and then is introduced to methane upon injection into the reaction cell. No peak at mass 153 was observed, indicating no $CpCoC_2H_5^+$ was formed. Therefore the peak observed at $m/z = 154$ in these experiments is almost certainly due to H_2 loss from $CpCo^+(CH_4)_2$.

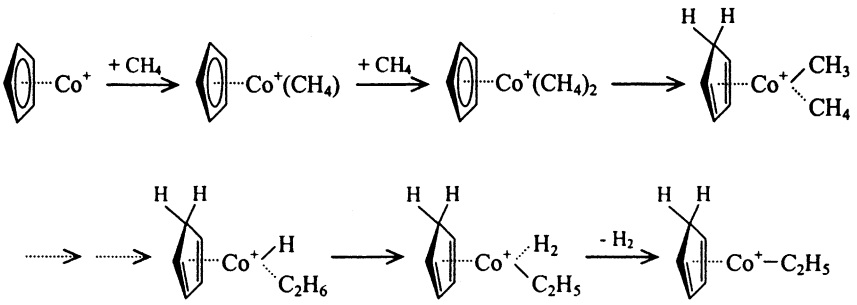

Scheme 1.

ligands to the Cp ring to form (c-C_5H_6)$Co^+(CH_3)(CH_4)$. We also located the last transition state associated with formation of the product complex (c-C_5H_6)$Co^+(H_2)(C_2H_5)$ from (c-C_5H_6)$Co^+(H)(C_2H_6)$. (In this transition state, a hydrogen atom is transferred from the C_2H_6 group to the H ligand via a multicenter structure composed of Co, C and two H atoms.) However, we could not locate an intermediate C–C coupling transition state that leads directly from (c-C_5H_6)$Co^+(CH_3)(CH_4)$ to (c-C_5H_6)$Co^+(H)(C_2H_6)$. Consequently, we were forced to explore other mechanistic options. The most promising involves the transfer of a hydrogen atom to the Cp ring followed by transfer of a methyl group and another hydrogen atom to the C_5-ring. This mechanism, along with energetics and a schematic potential energy surface are shown in Fig. 8.

As the DFT results shown in Fig. 8 indicate, the molecular complexes $CpCo^+(CH_4)$ and $CpCo^+(CH_4)_2$ are energetically stable species. The CH_4 ligand is bound by about 20 kcal/mol and some fraction of the nascent chemically activated $[CpCo^+(CH_4)]^*$ intermediate should be long-lived enough to add a second CH_4 group at the mTorr pressures of the MIKES experiments. A fraction of these $[CpCo^+(CH_4)_2]^*$ ions will lose H_2 before exiting the ion source, as observed in the equilibrium studies that occur at higher CH_4 pressures.

As shown in Fig. 8, the most stable product channel appears to be $CpCo^+(C_2H_6) + H_2$. However, the results of the CID experiments described above led us to consider alternative reaction pathways including the formation of (c-C_5H_6)Co^+–$C_2H_5 + H_2$ by a mechanism that directly involves the Cp ligand. This channel is exothermic by 1.2 kcal/mol and the various intermediates for the mechanism that must lie along the reaction pathway to form (c-C_5H_6)Co^+–$C_2H_5 + H_2$ all appear to be stable with respect to the $CoCp^+ + 2CH_4$ asymptote. The transition states for this mechanism are all slightly above the

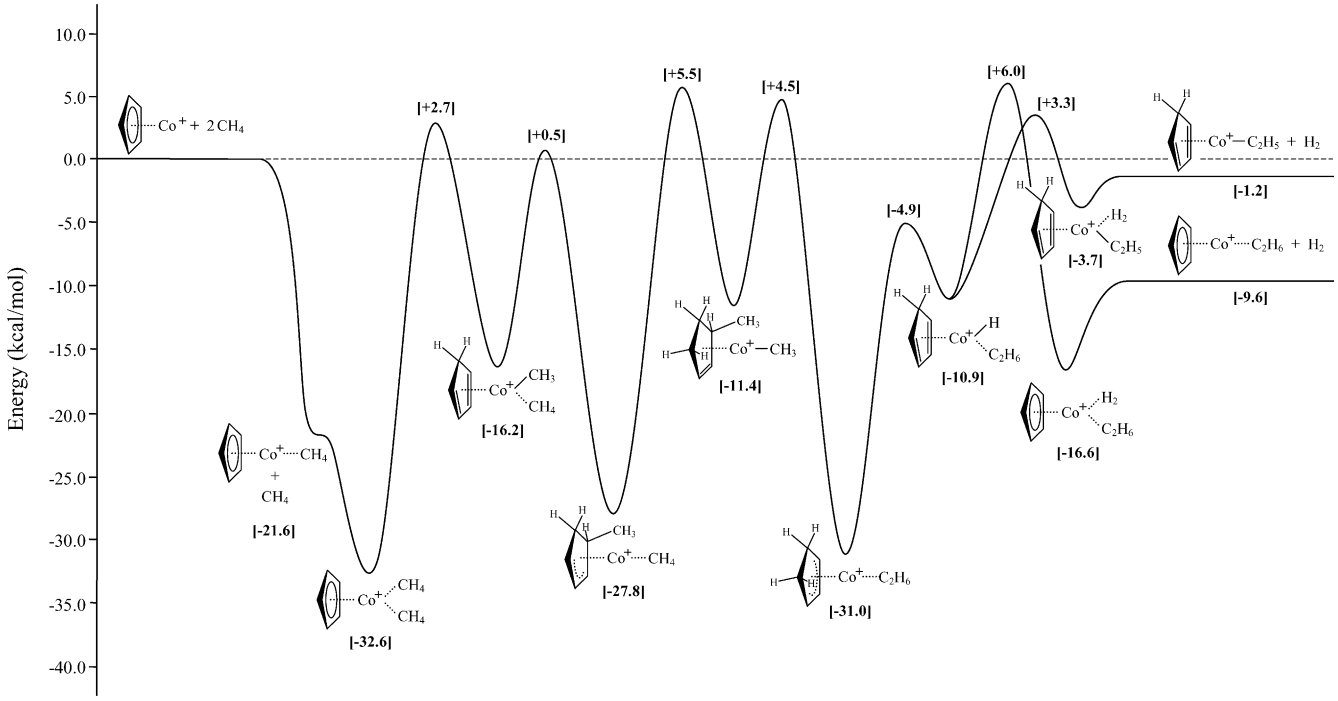

Fig. 8. Schematic potential energy surface at 0 K for the dehydrogenation of methane by $CoCp^+$ to form (c-C_5H_6)Co^+–C_2H_5 and $CpCo^+(C_2H_6)$. Calculated relative energies in kcal/mol are given in brackets below the reaction intermediates and at the transitions states.

$CoCp^+ + 2CH_4$ asymptotic energy (up to 5.5 kcal/mol) but given DFT's tendency to underestimate Co bond energies, these barriers may actually be below the reactant threshold. The significant stability of the $(C_6H_9)Co^+(CH_4)$ intermediate (−27.8 kcal/mol relative to reactants) points to this mechanism being reasonable for formation of $(c\text{-}C_5H_6)Co^+–C_2H_5$.

In contrast, theoretical calculations for intermediates that might be expected in formation of the ethane complex, $CpCo^+(C_2H_6)$, which do not involve hydrogen or methyl-group addition to the Cp ligand, such as $CpCo^+(CH_4)(CH_3)(H)$ and $CpCo^+(C_2H_6)(H)_2$, could not be converged and instead spontaneously reverted to corresponding stable species shown in Fig. 8. In fact, all species where the metal center was oxidized to the Co(IV) state, forming two covalent bonds while simultaneously maintaining its interaction with the C_5-ring, were found to be high in energy. The ethane complex can be formed from the $(c\text{-}C_5H_6)Co^+(H)(C_2H_6)$ intermediate but the transition state is 2.7 kcal/mol higher than for formation of the $(c\text{-}C_5H_6)Co^+–C_2H_5$ product from this same intermediate. This result suggests a significant competitive disadvantage for the formation of the ethane complex, explaining why $(c\text{-}C_5H_6)Co^+–C_2H_5$ formation is the favored reaction channel (Fig. 3b).

5. Conclusion

The clustering of H_2 and CH_4 to $CoCp^+$ was investigated by temperature-dependent equilibrium experiments. Measurement of enthalpy and entropy changes for these clustering reactions indicates that Co^+ can only accommodate two ligands in addition to the Cp ring. This experimental observation is confirmed by molecular geometries for $CpCo^+(H_2)_{1,2}$ and $CpCo^+(CH_4)_{1,2}$ determined by DFT. Experimental bond energies for the H_2 and CH_4 ligands were determined: $-\Delta H_0^\circ$ = 16.2, 16.8 and 0.9 kcal/mol for the first, second and third H_2 group and 24.1, 12.1 and 2.2 kcal/mol for the first, second and third CH_4 group clustering to $CoCp^+$. These values agree well with those calculated by DFT.

Experimental evidence, including temperature-dependent equilibrium studies, CID and KERDs, indicates that $CoCp^+$ is capable of eliminating H_2 from two methane ligands. In addition, the CID results, along with the theoretical investigation, indicate that the mechanism for this reaction directly involves the Cp ring. It should be emphasized that H and CH_3 groups must be transferred to the Cp ligand to allow the Co(II) center to form either Co–C or Co–H covalent bonds essential for the reaction to proceed. The alternative is for the cobalt center to be oxidized to Co(IV), a state far too high in energy for the reaction to proceed at thermal energies. Hence, the active participation of the C_5-ring is essential.

Acknowledgements

We gratefully acknowledge the support of the National Science Foundation under grant CHE-0140215. We also would like to thank Prof. Helmut Schwarz and Dr. Detlef Schröder of Technische Universität Berlin for helpful comments. And special thanks go to Prof. John Beynon without whom the ZAB would not have existed and this, and 91 other papers from our group, wouldn't have been possible.

References

[1] (a) K. Eller, H. Schwarz, Chem. Rev. 91 (1991) 1121;
(b) B.S. Freiser (Ed.), Organometallic Ion Chemistry, Kluwer Academic Publishers, Dordrecht, The Netherlands, 1996;
(c) C. Hall, R.N. Perutz, Chem. Rev. 96 (1996) 3125;
(d) A.E. Shilov, G.B. Shul'pin, Chem. Rev. 97 (1997) 2879;
(e) R.H. Crabtree, J. Chem. Soc., Dalton Trans. (2001) 2437;
(f) J.A. Labinger, J.E. Bercaw, Nature 417 (2002) 507.
[2] (a) J.E. Bushnell, P.R. Kemper, P. van Koppen, M.T. Bowers, J. Phys. Chem. A 105 (2001) 2216;
(b) F. Liu, R. Liyanage, P.B. Armentrout, J. Chem. Phys. 117 (2002) 132;
(c) X.-G. Zhang, P.B. Armentrout, J. Chem. Phys. 116 (2002) 5565;
(d) X.-G. Zhang, C. Rue, S.-Y. Shin, P.B. Armentrout, J. Chem. Phys. 116 (2002) 5574;
(e) M.J. Manard, J.E. Bushnell, S.L. Bernstein, M.T. Bowers, J. Phys. Chem. A 106 (2002) 10027.
[3] (a) J.J. Carroll, K.L. Haug, J.C. Weisshaar, M.R.A. Blomberg, P.E.M. Siegbahn, M. Svensson, J. Phys. Chem. 99 (1995) 13955;
(b) J.J. Carroll, J.C. Weisshaar, P.E.M. Siegbahn, C.A.M. Wittborn, M.R.A. Blomberg, J. Phys. Chem. 99 (1995) 14388;
(c) J.J. Carroll, J.C. Weisshaar, J. Phys. Chem. 100 (1996) 12355;
(d) A.M.C. Wittborn, M. Costas, M.R.A. Blomberg, P.E.M. Siegbahn, J. Chem. Phys. 107 (1997) 4318.
[4] J. Allison, R.B. Freas, D.P. Ridge, J. Am. Chem. Soc. 101 (1979) 1332.
[5] (a) A.H. Janowicz, R.G. Bergman, J. Am. Chem. Soc. 104 (1982) 352;
(b) J.K. Hoyano, W.A.G. Graham, J. Am. Soc. 104 (1982) 3723;
(c) W.D. Jones, F.J. Feher, J. Am. Chem. Soc. 104 (1982) 4240;
(d) A.H. Janowicz, R.G. Bergman, J. Am. Chem. Soc. 105 (1983) 3929;
(e) J.K. Hoyano, A.D. McMaster, W.A.G. Graham, J. Am. Chem. Soc. 105 (1983) 7190;
(f) T. Sakakura, T. Sodeyama, K. Sasaki, K. Wada, M. Tanaka, J. Am. Chem. Soc. 112 (1990) 7221.
[6] B.A. Arndtsen, R.G. Bergman, T.A. Mobley, T.H. Peterson, Acc. Chem. Res. 28 (1995) 154.
[7] (a) B.L. Tjelta, P.B. Armentrout, J. Am. Chem. Soc. 117 (1995) 5531;
(b) B.L. Tjelta, P.B. Armentrout, J. Am. Chem. Soc. 118 (1996) 9652;
(c) P.B. Armentrout, B.L. Tjelta, Organometallics 16 (1997) 5372.
[8] A. Chen, H. Chen, S. Kais, B.S. Freiser, J. Am. Chem. Soc 119 (1997) 12879.
[9] (a) J.E. Bushnell, P.R. Kemper, P. Maitre, M.T. Bowers, J. Am. Chem. Soc. 116 (1994) 9710;
(b) P.A.M. van Koppen, J.K. Perry, P.R. Kemper, J.E. Bushnell, M.T. Bowers, Int. J. Mass Spectrom. 187 (1999) 989.
[10] (a) D. Wang, R.R. Squires, J. Am. Chem. Soc. 109 (1987) 7557;
(b) R. Stepnowski, J. Allison, J. Am. Chem. Soc. 111 (1989) 449;

(c) C.S. Christ Jr., J.R. Eyler, D.E. Richardson, J. Am. Chem. Soc. 112 (1990) 596;
(d) G. Innorta, S. Torroni, A. Maranzana, G. Tonachini, J. Organomet. Chem. 626 (2001) 24;
(e) H.C.M. Byrd, C.M. Guttman, D.P. Ridge, J. Am. Soc. Mass Spectrom. 14 (2003) 51.
[11] (a) D.B. Jacobson, B.S. Freiser, J. Am. Chem. Soc. 107 (1985) 7399;
(b) D. Ekeberg, E. Uggerud, H.-Y. Lin, K. Sohlberg, H. Chen, D.P. Ridge, Organometallics 18 (1999) 40.
[12] J. Chowdhury, K. Fouhy, A. Shanley, Chem. Eng. 103 (1996) 35.
[13] C.J. Carpenter, P.A.M. van Koppen, M.T. Bowers, J.K. Perry, J. Am. Chem. Soc. 122 (2000) 392.
[14] (a) C.L. Haynes, P.B. Armentrout, J.K. Perry, W.A. Goddard, J. Phys. Chem. 99 (1995) 6340;
(b) Q. Zhang, P.R. Kemper, S.K. Shin, M.T. Bowers, Int. J. Mass Spectrom. 204 (2001) 281.
[15] (a) R. Tonkyn, M. Ronan, J.C. Weisshaar, J. Phys. Chem. 92 (1988) 92;
(b) R. Georgiadis, E.R. Fisher, P.B. Armentrout, J. Am. Chem. Soc. 111 (1989) 4251.
[16] (a) P.R. Kemper, M.T. Bowers, J. Am. Soc. Mass Spectrom. 1 (1990) 197;
(b) P.R. Kemper, P. Weis, M.T. Bowers, Int. J. Mass Spectrom. Ion Process. 160 (1997) 17.
[17] R.P. Morgan, J.H. Beynon, R.H. Bateman, B.N. Green, Int. J. Mass Spectrom. Ion Phys. 28 (1978) 171.
[18] B.A. Rumpf, P.J. Derrick, Int. J. Mass Spectrom. Ion Process. 82 (1988) 239.
[19] (a) A.D. Becke, Phys. J. Chem. Phys. 98 (1993) 5648;
(b) C. Lee, W. Yanz, R.G. Parr, Phys. Rev. B 37 (1988) 785. Implemented as described in B. Miehlich, A. Savin, H. Stoll, H. Preuss, Chem. Phys. Lett. 157 (1989) 200.
[20] JAGUAR 5.0, Schrodinger, Inc., Portland, OR, 1998.
[21] (a) P.J. Hay, W.R. Wadt, J. Chem. Phys. 82 (1985) 299;
(b) W.J. Hehre, J.A. Pople, J. Chem. Phys. 56 (1972) 4233;
(c) R. Krishnan, J.S. Binkley, R. Seeger, J.A. Pople, J. Chem. Phys. 72 (1980) 650;
(d) M.J. Frisch, J.A. Pople, J.S. Binkley, J. Chem. Phys. 80 (1984) 3265.
[22] M.A. Hanratty, J.L. Beauchamp, A.J. Illies, P. van Koppen, M.T. Bowers, J. Am. Chem. Soc. 110 (1988) 1.
[23] (a) D.B. Jacobson, B.S. Freiser, J. Am. Chem. Soc. 105 (1983) 5197;
(b) P.B. Armentrout, J.L. Beauchamp, Acc. Chem. Res. 22 (1989) 315.
[24] (a) P.R. Kemper, J. Bushnell, G. von Helden, M.T. Bowers, J. Phys. Chem. 97 (1993) 52;
(b) C.L. Haynes, P.B. Armentrout, Chem. Phys. Lett. 249 (1996) 64.
[25] C.W. Bauschlicher Jr., P. Maitre, J. Phys. Chem. 99 (1995) 3444.